Computational and Theoretical Chemistry 1069 (2015) 105–111

Contents lists available at ScienceDirect

Computational and Theoretical Chemistry

journal homepage: www.elsevier.com/locate/comptc

Theoretical study of the ground state of $(EDO\text{-}TTF)_2PF_6$

Gerrit-Jan Linker [a,*], Piet Th. van Duijnen [a], Paul H.M. van Loosdrecht [b], Ria Broer [a]

[a] Theoretical Chemistry, Zernike Institute for Advanced Materials, University of Groningen, The Netherlands
[b] Physics Institute 2, University of Cologne, Germany

ARTICLE INFO

Article history:
Received 29 May 2015
Received in revised form 6 July 2015
Accepted 7 July 2015
Available online 20 July 2015

Keywords:
$(EDO\text{-}TTF)_2PF_6$
Ground state
Closed shell
Open shell
Ab initio

ABSTRACT

In this paper we present a theoretical study of the nature of the ground state of the $(EDO\text{-}TTF)_2PF_6$ charge transfer salt by using *ab initio* quantum chemical theory for clusters in vacuum, for embedded clusters and for the periodic system. Exemplary for other organic charge transfer systems, we show that by using a relatively low level of theory it is possible to obtain a good understanding of the electronic structure of the ground state. An assessment is made of the proximity of the triplet, the open shell singlet and the closed shell singlet states of $(EDO\text{-}TTF)_2PF_6$. Our calculations reveal also that several charge ordered states are very close in energy.

1. Introduction

The good conduction in many organic charge transfer (CT) salts is commonly considered to be due to the delocalisation of radical electrons. For example this is the case in the highly conducting TTF-TNCQ compound in which both constituent molecules, tetrathiafulvalene TTF^+ and tetracyanoquinodi-methane $TNCQ^-$, can be considered as radical ions [1]. In the $(EDO\text{-}TTF)_2PF_6$ CT salt, neutral ethylenedioxytetrathiafulvalene $EDO\text{-}TTF_2$ dimers become cations after transferring an electron to the acceptor molecule hexafluorophosphate (PF_6). The acceptor molecule is a radical in its neutral configuration and becomes closed shell after accepting an electron. Interacting cation dimers also occur in the well known and iso-structural Fabre and Bechgaard salts. These materials are sometimes classed radical cation salts. In this paper we address the question whether in $(EDO\text{-}TTF)_2PF_6$ the ground state of two neighbouring $(EDO\text{-}TTF)_2^+$ cations can be characterised best as an open shell singlet, as an open shell triplet or as a closed shell singlet ground state.

$(EDO\text{-}TTF)_2PF_6$ exhibits a metal-insulator transition [2] at $T_c = 278$ K. This is classed a first order transition, because the magnetic susceptibility χ displays hysteresis over the transition. The high temperature (HT) susceptibility is $\chi_{HT} = 2.5 \cdot 10^{-4}$ emu/mol, and it vanishes at low temperature [2] (LT). Compared to the metallic phase at HT, the unit cell in the insulating phase at LT is doubled. The number of EDO-TTF molecules in the unit cell is two at HT, and it is four at LT. This transition is thought to be due to the interplay of multiple instabilities such as a connected [3] charge ordering and ordering of molecular deformations, dimerisation of EDO-TTF molecules, ordering and disorder of PF_6 molecules [2]. The EDO-TTF donor molecules arrange in columns that are separated by the PF_6 acceptor molecules. Due to the CT to PF_6 molecules, electron holes are created in the EDO-TTF molecular stacks. In the HT crystal the positive charge is evenly distributed over the equidistant EDO-TTF molecules [4]. In the LT crystal, EDO-TTF molecules adopt one of two molecular geometries. Neutral molecules are bent molecules while the full charge is borne by planar EDO-TTF molecules [4,21]. The dimerisation leads to a larger distance between adjacent bent molecules. Despite this difference, both the LT and HT crystal can be thought of as containing $(EDO\text{-}TTF)_2^+$ radicals. Experimentally no magnetic state has been found, which seems to make the occurrence for radical electrons unlikely. We explore the diradical character of the ground state from a first principles quantum chemical view point. Diradical character is important for electronic, optical and magnetic properties [5]. The small Pauli paramagnetic susceptibility observed at high temperatures originates from the metallic nature of the high temperature state. A magnetic ground state [6] is found at low temperature in the related Fabre salt that contains the tetra methyl derivative of TTF: $TMTTF_2PF_6$. The temperature dependence of the magnetic susceptibility in this material [7] shows no feature due to the transition to a charge ordered state with alternating neutral and positively charged TMTTF molecules in which the inversion symmetry is broken. Interestingly, as is recently revealed by ESR measurements [7], in this state in-equivalent antiferromagnetic TMTTF chains coexist.

* Corresponding author.
E-mail address: g.j.linker@rug.nl (G.-J. Linker).

http://dx.doi.org/10.1016/j.comptc.2015.07.009
2210-271X/

Embedded spin-unrestricted density functional theory (DFT) calculations on the HT crystal by Iwano and Shimoi [8,9] indicate that an antiferromagnetic spin-polarised state is slightly lower in energy than the closed shell solution. Their recent DFT study [10] on the relaxation mechanism of the photo induced phase is also noteworthy. Filatov [11] obtained spin-polarised solutions both in the HT and in the LT system from embedded ensemble DFT calculations. Analysing the interactions between unpaired electron spins, he assigned the LT system to be diamagnetic and the HT system to be anti-ferromagnetic. Spin-unrestricted calculations often yield broken spin-symmetry solutions [12] that are slightly lower in energy than the solution in which all electron spins pair. In Hartree–Fock (HF) theory this situation is known as triplet instability [13].

Our study is mainly a ground state investigation, but we also pay attention to the lowest excited states of $(EDO\text{-}TTF)_2PF_6$. The optical conductivity spectrum [14,15] at HT shows one peak at 1200 cm^{-1} (0.15 eV; 3 kcal/mol) with a dip at slightly higher energy that is attributed to vibronic coupling. Instead, the spectrum at LT shows two charge transfer peaks, one (CT1) around 4500 cm^{-1} (0.56 eV; 13 kcal/mol) and one (CT2) around 11150 cm^{-1} (1.4 eV; 32 kcal/mol). CT1 was assigned to a $D^+D^0 \rightarrow D^0D^+$ transition and CT2 to a $D^+D^+ \rightarrow D^{2+}D^0$ transition where D denotes an EDO-TTF molecule. The $(EDO\text{-}TTF)_2PF_6$ material is also known for its very highly photon sensitive photo-induced (PI) phase transition in which it is sufficient to excite only one in 500 EDO-TTF molecules [20,21]. The spectrum for the PI state is different from both the HT and LT spectra. It is considered that the conducting PI state has a 0101 charge ordering of the four EDO-TTF molecules of each unit cell [22].

This paper is organised as follows. After some theoretical considerations and computational details, the results of complete active space SCF (CASSCF) and complete active space CI (CASCI) calculations on a tetramer cluster in vacuum are presented. The electrostatic effect of the crystal environment is taken into account in embedded cluster calculations while the crystal is treated in its entirety in periodic calculations.

Next, for the analysis of the CASSCF calculations, the low-lying electronic configurations are studied with spin-restricted (open shell) Hartree–Fock (RHF/ROHF). Finally, spin-unrestricted Hartree Fock (UHF) cluster calculations are presented that serve as a reference for periodic UHF calculations.

2. Theoretical considerations

Considering a single tetramer unit cell containing two $(EDO\text{-}TTF)_2^+$ cations and two closed shell PF_6^- anions, the question can be posed which ansatz is better, one in which the two electrons of the dimers are described by a common tetramer orbital, or one in which they each occupy a different orbital. The simplest possible representation of the system is by using a single configuration state function (CSF). Fig. 1 shows in cartoons, three tetramer cluster ground states that are likely in such a one-configurational approach in a two orbital model in which each dimer electron is schematically described by a local orbital. The tetramer cluster wave functions for the CS, OS singlet and T states can be formulated. An orthonormal local basis $\{a, b\}$ is used where $a = (g + u)/\sqrt{2}$ and $b = (g - u)/\sqrt{2}$ with a and b predominantly localised on each of the dimers, and in which $\{g, u\}$ is a set of orthonormal inversion symmetry adapted (SA) orbitals. In any case, any wave function in the SA basis $\{g, u\}$ can be written in the local basis $\{a, b\}$ and *vice versa*. In the case of strong interaction, a description in the SA basis is appealing and in the extreme of weak interaction, the description by the local basis is most attractive. In intermediate cases it is *a priori* not clear which set of orbitals offers the best single CSF description. In fact, as we will show in this paper, the $(EDO\text{-}TTF)_2PF_6$ material represents such a case.

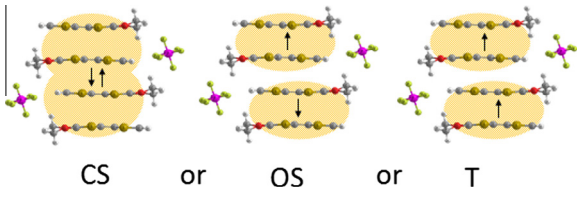

Fig. 1. Depictions of possible electronic configurations of two $EDO\text{-}TTF_2^+$ dimers: sharing an orbital in a closed shell (CS) configuration or in an open shell with a singlet (OS) or triplet (T) coupling.

It is useful for the analysis of the results of our calculations to define the relevant states as an orthonormal set of CSFs in terms of in both basis sets, see Tables 1a and 1b. In the case of strong interaction of *a* and *b*, the ${}^1_{CS}\psi(g,g)$ CS wave function is expected to be lowest in energy. In the weak interaction limit, the open shell wave functions, in which each electron is assigned to a different local orbital, are expected to describe the ground state best.

The open shell $M_s = 1$ triplet determinant $|gu|$ $(= -|ab|)$ is a proper eigenfunction of $\widehat{S}^2$ but we chose to use the two determinantal description of the $M_s = 0$ triplet component ${}^3_{OS}\psi(g,u)$ $(= -{}^3_{OS}\psi(a,b))$. In the local basis, the same two determinants $|a\bar{b}|$ and $|b\bar{a}|$ used in ${}^3_{OS}\psi(a,b)$ can be used to construct the OS singlet ${}^1_{OS}\psi(a,b)$ (Table 1b). Single determinants $|g\bar{u}|$ and $|a\bar{b}|$ are not eigenfunctions of $\widehat{S}^2$, so open shell singlet systems cannot be properly described by one determinant. When using spin-unrestricted HF (UHF) theory a one-determinantal model is used nonetheless and that has implications. Within the two orbital model, a single determinant spin-unrestricted $M_s = 0$ wave function can be written as a mixture of singlet and triplet wave functions, e.g. in the SA basis $|a\bar{b}| = [{}^1_{OS}\psi(a,b) + {}^3_{OS}\psi(a,b)]/\sqrt{2}$. It is intermediate between ${}^1_{OS}\psi$ and ${}^3_{OS}\psi$ and the expectation value of $\widehat{S}^2$ becomes $\langle\widehat{S}^2\rangle = 1$. The orbitals can be seen as average orbitals optimised for an average of singlet and triplet. Orbital overlap can lead to wave functions with $\langle\widehat{S}^2\rangle \neq 1$. In these cases, the UHF wave function contains open shell singlet and triplet components that are mixed to an *a priori* unknown amount. When $\langle\widehat{S}^2\rangle \neq 1$, the energy for a particular electronic configuration can best be obtained with ROHF.

Considering the crystal, singlet unit cells can combine in various ways. CS unit cells combine to a CS crystal ground state. When considering a multitude of OS singlet unit cells, the open shell electrons can remain open shell in the crystal or, (partially) couple closed shell. When a crystal is described using a

Table 1a
CSFs in the SA basis and their local basis equivalents.

CSF		SA and local basis
${}^1_{CS}\psi(g,g)$	=	$\|g\bar{g}\| \doteq (\|a\bar{a}\| + \|b\bar{b}\| + (\|a\bar{b}\| + \|b\bar{a}\|))/2$
${}^1_{CS}\psi(u,u)$	=	$\|u\bar{u}\| \doteq (\|a\bar{a}\| + \|b\bar{b}\| - (\|a\bar{b}\| + \|b\bar{a}\|))/2$
${}^1_{OS}\psi(g,u)$	=	$(\|g\bar{u}\| + \|u\bar{g}\|)/\sqrt{2} \doteq (\|a\bar{a}\| - \|b\bar{b}\|)/\sqrt{2}$
${}^3_{OS}\psi(g,u)$	=	$(\|g\bar{u}\| - \|u\bar{g}\|)/\sqrt{2} \doteq (\|b\bar{a}\| - \|a\bar{b}\|)/\sqrt{2}$

Table 1b
CSFs in the local basis and their SA basis equivalents.

CSF		Local and SA basis
${}^1\psi(a,b)$	=	$(\|a\bar{a}\| + \|b\bar{b}\|)/\sqrt{2} \doteq (\|g\bar{g}\| + \|u\bar{u}\|)/\sqrt{2}$
${}^1_{OS}\psi(a,b)$	=	$(\|a\bar{b}\| + \|b\bar{a}\|)/\sqrt{2} \doteq (\|g\bar{g}\| - \|u\bar{u}\|)/\sqrt{2}$
${}^3_{OS}\psi(a,b)$	=	$(\|a\bar{b}\| - \|b\bar{a}\|)/\sqrt{2} \doteq (\|u\bar{g}\| - \|g\bar{u}\|)/\sqrt{2}$

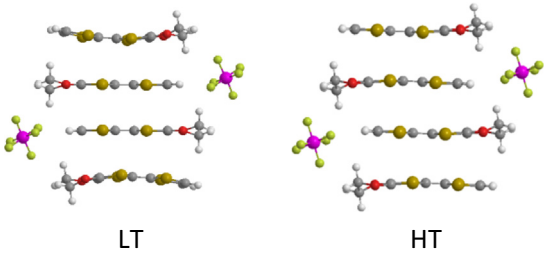

Fig. 2. Tetramer "unit cell" of the low temperature (LT) crystal and the high temperature (HT) crystal.

multi-configurational approach, the character of the resulting wave function is unlikely to be purely CS or OS singlet.

3. Computational details

The geometries used for all calculations are derived from the crystal structures obtained by X-ray diffraction by Ota et al. [2], at low (260 K) and high temperature (300 K). For our cluster calculations we follow common practise and use these geometries. We use a stoichiometric, centro-symmetric "unit cell" cluster containing a single stack of four EDO-TTF molecules and two PF_6 molecules (see Fig. 2). Our choice for planar (bent) inner (outer) EDO-TTF molecules leads to a pattern of molecular charges that corresponds reasonably well to what is experimentally observed for the LT structure. This is also partly due to the positioning of the centro-symmetrical anions.

All (embedded) cluster calculations were performed using the 6-31G** basis set [23]. The Gamess-UK package [24] was used for RHF and ROHF calculations. CASSCF, UHF and RHF calculations were done by applying Cholesky integral decomposition, using the Molcas package [25]. In relevant cases, state average CASSCF calculations were performed. Periodic restricted and unrestricted HF calculations were performed with the CRYSTAL09 package [26]. The 6-21G basis set [27] was used for these calculations. We performed calculations of the internal energy of the system and we chose to not include entropic effects. These effects may play a role in this system considering the unit cell doubling involved in the phase transition. Charge analysis was performed using Mulliken population analysis [28]. Henceforth we use the molecular HOMO and LUMO, designations also for tetramer cluster orbitals.

4. CASSCF cluster calculations

Table 2 summarises the lowest singlet and triplet CASSCF states obtained for the LT and HT tetramer clusters in vacuum. The CASSCF wave function of lowest energy that we calculated consists of g^2 and u^2 determinants, and we interpret it as a more or less equal mixture of ${}^1_{CS}\psi = |g\bar{g}|$ and ${}^1_{OS}\psi = (|g\bar{g}| - |u\bar{u}|)/\sqrt{2}$, i.e. a situation between closed shell singlet and open shell singlet. A CAS(6,4) calculation with six electrons in four orbitals (HOMO-2 to LUMO) is of particular interest. The CAS(6,4) treats the four frontier tetramer cluster orbitals, that are built from all four molecular EDO-TTF HOMOs, on equal footing (for the RHF orbitals see Table 6). The stability of the CAS(6,4) solution with respect to the size of the CAS space is checked by adding a substantial number of virtual orbitals to the active space in a CAS(6,14) calculation and in a CAS(6,29) calculation. Also a minimal CAS(2,2) calculation was performed.

The singlet state is in all calculations lower in energy than the triplet state (see Table 2). The CASSCF singlet-triplet splitting is of the order of 10 (4) kcal/mol in the LT (HT) crystal. Due to the stronger interaction between the electron spins at LT, where the distance between the $(EDO\text{-}TTF)_2$ dimers is smaller, the splitting is largest. For the triplet, the single g^1u^1 configuration of the small CAS(2,2) is also dominant in the CAS(6,4). In this CAS space the singlet wave function has (predominantly) contributions from one g^2 and one u^2 configuration. When extending the CAS space to CAS(6,14) and CAS(6,29), about 7–8% other configurations mix into the wave functions.

Table 2
Lowest singlet and triplet CASSCF energies in kcal/mol relative to the RHF CS energy of the LT and HT cluster.

CAS	S_{0g}		T_{1u}	
	E_{LT}	E_{HT}	E_{LT}	E_{HT}
CAS(2,2)	−14.5	−18.2	−4.7	−14.5
CAS(6,4)	−15.7	−18.4	−4.9	−14.6
CAS(6,14)	−51.4	−55.5	−35.8	−51.2
CAS(6,29)	−54.5	−57.1	−43.6	−53.0

Analysis of the singlet CASSCF wave function can be found in Table 3. For all active spaces the same qualitative picture emerges and we restrict our discussion to the analysis of the CASSCF(6,4) results. In the LT (HT) clusters, the $1g^21u^22g^22u^0$ configuration is the dominant contribution with a CI coefficient of 0.92 (0.86). A $1g^01u^22g^22u^2$ configuration mixes in. For the details of these orbitals we refer to the RHF section of this paper. The natural orbital population shows the configuration mixing as $(n_g, n_u) = (1.7, 0.3)$ in the LT cluster and $(n_g, n_u) = (1.5, 0.5)$ in the HT cluster. It shows that the wave function for the LT (HT) cluster has 70% (50%) closed shell character: a pure open shell singlet (${}^1_{OS}\psi(a,b)$ in Table 1b) would have yielded a $(n_g, n_u) = (1, 1)$ occupation. From a spatial analysis of the natural orbitals it becomes clear that there is localisation of the hole orbitals in the interior of the cluster. Mulliken charge analyses also show the 0110 charge ordering pattern, in which each number represents the charge of a EDO-TTF molecule in the tetramer unit cell. The inner molecules adopt 97% (90%) of the charge hole in the LT (HT) cluster. In both clusters, the CT of each $(EDO\text{-}TTF)_2$ dimer to PF_6 is 0.94 electrons.

An interpretation of the multi-configurational wave functions in terms of the closed shell RHF wave function and its excited configurations is possible by performing a CASCI calculation in which the CI coefficients are obtained without optimising the RHF orbitals. Compared to the CASSCF solution, the only difference for the CASCI solution in each cluster is a modest (3 kcal/mol) higher total energy. With regards to the contribution of RHF configuration to the correlated wave function the same picture emerges.

It is noted that the charge ordering pattern is dictated by the choice of the cluster and its geometry. Our results might be sensitive to small variations in the geometry that fall within the accuracy of the X-ray diffraction experiments from which our geometries were obtained. In particular, we recognise that in these experimentally observed geometries there is some thermal disorder and the hydrogen positions are not observed directly. With

Table 3
CASSCF wave function analysis for the singlet state of the LT and cluster for various CAS spaces. The CI coefficients of the g^2 and u^2 configurations are given. The natural orbital populations (NO occ.) give an indication of the electron transfer from the g^2 configuration.

CAS	LT				HT			
	CI coeff.		NO occ.		CI coeff.		NO occ.	
	g^2	u^2	n_g	n_u	g^2	u^2	n_g	n_u
CAS(2,2)	0.911	−0.413	1.66	0.34	0.858	−0.513	1.47	0.53
CAS(6,4)	0.917	−0.390	1.70	0.32	0.862	−0.505	1.51	0.50
CAS(6,14)	0.884	−0.371	1.69	0.30	0.834	−0.476	1.50	0.49
CAS(6,29)	0.887	−0.369	1.70	0.29	0.836	−0.475	1.51	0.49

our cluster choice (Fig. 2) the charge ordering pattern for the LT crystal corresponds to the experimentally observed (from infrared and Raman spectra [15] and also from charge densities obtained from X-ray data [4]) charge ordering in the crystal, however at HT a ½½½½ distribution is observed. The fact that positive charges get stabilised in the interior of the cluster is a consequence of the choice of using a cluster model. Firstly, the HOMO in a neutral tetramer stack is localised mostly on the two interior molecules. Moreover, compared to charge on a cluster surface, charge in the cluster interior is surrounded by more electron density that can be polarised due to the charge. We think this leads to higher induction interactions that stabilise the system. In contrast to the cluster model, calculations with a periodic model for the HT crystal shows that the charge hole is delocalised (*vide infra*). In studies on the Cope rearrangement [16,17] and on the benzyne biradical [18,19], inclusion of dynamical correlation effects of the inactive valence electrons was found to reduce the diradical character of the wave function. Since in our calculations we did not include these effects, it is not unlikely that our results overestimate the open shell character of the EDO-TTF molecules.

5. Embedded cluster CASSCF calculations

The electrostatic effect of the direct cluster environment on the CASSCF calculations is studied by embedding the cluster in point charges. In this section, we denote the tetramer cluster as D_4A_2 where D and A denote donor and acceptor molecules respectively. We increased the size of the clusters further by including up to ten nearest neighbour PF_6 molecules into the cluster (Fig. 3).

The atomic charges, used to represent molecules in the embedding, were obtained from molecular calculations in vacuum. They preserve the molecular multipole field [29], and their use is therefore expected to give proper electrostatic intermolecular interactions. The central tetramer, treated quantum mechanically, was surrounded by several embedding unit cells. In the direction of the long molecular axis and in the direction in which the EDO-TTF molecules stack, a single unit cell was used as embedding. In the direction of the short molecular axis we used two unit cells as embedding so the overall system is approximately cubic. In embedded DFT calculations, Iwano and Shimoi [9] found that three layers are needed to reproduce the crystal field, hence our scheme should be seen as a first order embedding. In the next section the crystal is described in its entirety, and the present embedded calculations serve only as an assessment of the role of electrostatic effects of the environment on the electronic structure.

The results of the embedded cluster CASSCF(6,14) calculations (Table 4) are similar to our vacuum results. The inclusion of the crystal field as well as the inclusion of additional anions has a negligible effect on the relative CASSCF energies and on the CI coefficients. It shows that our choice of tetramer cluster model, used in the vacuum calculations, is legitimate (Fig. 2). Unlike all other clusters at HT and LT in Table 4, it was not possible to obtain a triplet state at HT for the embedded D_4A_2 cluster with the 0110 charge ordering pattern using the (6,4) CAS space. Instead, it was obtained using a CAS(6,6). In Table 4 we used the CAS(6,14) results for easy comparison to the CI coefficient in vacuum (Table 3). The charge ordering obtained for all results in Table 4 is 0110.

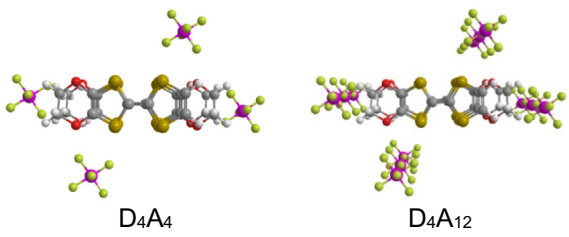

Fig. 3. The D_4A_4 and D_4A_{12} clusters (see text) built by adding two and ten PF_6 anions to the D_4A_2 cluster. These clusters were embedded in point charges (not shown).

Table 4
CASSCF Singlet–Triplet (E_T–E_S) splittings in kcal/mol of several donor (D)–acceptor (A) clusters in vacuum and in an embedding (see text).

		Vacuum	Embedded		
		D_4A_2	D_4A_2	D_4A_4	D_4A_{12}
LT	E_T–E_S	10.8	10.0	9.8	9.8
	g^2 CI coeff.	0.917	0.911	0.910	0.910
HT	E_T–E_S	3.8	3.1	3.5	3.5
	g^2 CI coeff.	0.862	0.834	0.862	0.863

For the small D_4A_2 cluster we checked whether a polarisable embedding affects the distribution of the positive charge. For this we obtained induced dipoles on all atomic positions from a fully classical calculation using the DRF90 software [30] on the cluster with embedding as described above. Subsequent CASSCF calculations for the singlet state on the cluster embedded with point charges and with the induced dipoles, shows negligible effects on the CI coefficients and on the molecular charges. When repeating the procedure for an embedded D_4^{2+} cluster, also a 0110 charge ordering was obtained.

The richness of the electronic structure of this material is shown by the several degenerate states that we could obtain for the embedded D_4A_2 cluster with the HT geometry. At −1 kcal/mol a triplet state with a CO 0101 was obtained with a corresponding singlet at 0 kcal/mol (energies relative to the singlet CAS(6,4) state with a CO of 0110). State average calculations over three states, both for singlet and for triplet, showed a singlet state at +2 kcal/mol and a triplet at +3 kcal/mol with a CO of ½½½½. Notably, these states are lower in energy than the first excited singlet state with a CO of 0110 which was found at +20 kcal/mol using a state average over two states.

6. Periodic calculations on the crystal

In periodic calculations the whole crystal is treated explicitly. However, calculations are currently only feasible at the HF and DFT levels of theory. Similar to the embedded cluster calculations, several states that are close in energy are found (Table 5) using periodic Hartree–Fock calculations. The proximity of these UHF and RHF states indicates that several states compete. The CT from $(EDO\text{-}TTF)_2$ to PF_6 is lower than in the cluster calculations. A CT of 0.76 (0.81) per PF_6 molecule in the LT (HT) crystal is calculated and it does not depend on the M_s value used, nor on the CO pattern obtained, nor on our choice of method.

As indicated in Table 5, given a CO pattern, the same molecular charges and charge ordering were obtained in the different calculations. The charge localisation in the HT system that we observed in the cluster calculations does not occur in the periodic system. Meaningful comparison is possible between states that have the same CO and CT because the electrostatics are the same. The obtained results for the experimentally observed charge ordering pattern at LT and HT (marked in grey), show triplet instability. In both crystals there are $M_s = 0$ UHF states lower in energy than the RHF state indicating that the true ground state has multi-determinantal character. All calculated states correspond to band insulators, except the RHF state at HT with the 1½½½½ charge distribution which is a band conductor. Because the $M_s = 0$ and $M_s = 1$ states are close in energy, and also considering the severe spin contamination in our UHF cluster calculations (*vide infra*), it is very likely that the $M_s = 0$ UHF state is close to triplet.

Table 5
Periodic RHF and UHF states. The results for the experimentally observed CO pattern at LT and HT are marked grey. Energy E in kcal/mol and are relative to the RHF energy for the experimentally observed CO pattern in both crystals.

	CO:	0110		0101		½½½½	
		E	CO	E	CO	E	CO
			-0.06				
			0.82				
			0.82				
LT	RHF	0	-0.06				
			-0.06		-0.07		0.38
			0.82		0.77		0.38
	UHF		0.82		0.00		0.38
	M_s=0	-16.4	-0.06	-10.9	0.82	0.7	0.38
			-0.06		-0.07		0.38
			0.82		0.77		0.38
	UHF		0.82		0.00		0.38
	M_s=1	-12.0	-0.06	-10.8	0.82	1.0	0.38
			0.08				0.41
			0.82				0.41
			0.82				0.41
HT	RHF	-4.7	0.08			0.0	0.41
					-0.02		0.40
					0.83		0.40
	UHF				-0.02		0.40
	M_s=0			-1.9	0.83	-1.4	0.40
					-0.02		0.40
					0.83		0.40
	UHF				-0.02		0.40
	M_s=1			-1.8	0.83	-1.3	0.40

Unfortunately it was not possible to obtain a value for the total spin per unit cell in these calculations and we therefore do not know the extent of spin contaminations. We found a RHF solution in the HT crystal with a CO pattern 0110 that is nearly 5 kcal/mol lower than the state with the experimentally observed charge distribution of ½½½½. It shows the instability of the system towards other charge orderings. A similar instability is observed in UHF results for both crystals, in which the 0101 CO was found. UHF states could be found at lower energy than the RHF state. The $M_s = 0$ and $M_s = 1$ 0101 states are very close in energy, which hints to a ferromagnetic state. Remarkable is that UHF solutions exist for the LT crystal with a ½½½½ charge distribution. Both bent and planar molecules adopt the same amount of charge hole in these solutions. It is very likely that there is a manifold of states with the 0110, 0101 and ½½½½ charge distribution patterns that are close in energy.

We will shortly publish a detailed study of the spin-restricted periodic results, performed both with HF theory and DFT, and we refer to this publication for further information and analysis of the electronic band structure.

7. RHF and ROHF calculations on the tetramer cluster

To support the analysis of the (embedded) cluster calculations, results from RHF and ROHF cluster calculations are presented. The four frontier orbitals of the cluster, shown in Table 6, are linear combinations of the highest occupied molecular orbitals (HOMOs) of the four EDO-TTF monomers. The tetramer HOMO-2 is the fully bonding combination and the tetramer LUMO is fully anti-bonding. These orbitals have very small amplitude on the PF_6 molecules. The CT to PF_6 is the same as in the CASSCF calculations. The charge hole localisation on the inner molecules is 95% (85%) in the LT (HT) geometry, which gives a charge ordering pattern of 0110 in both cases. This is 2% (5%) less compared to the CASSCF results for the LT (HT) geometry.

Table 6
RHF charge ordering (CO) and CS frontier orbitals for the LT and HT unit cells. Orbital energies ε are in hartree.

Orbital	LT		HT	
2*u* LUMO	$\varepsilon = -0.1279$	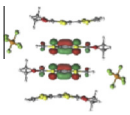	$\varepsilon = -0.1422$	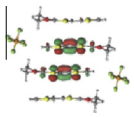
2*g* HOMO	$\varepsilon = -0.2683$	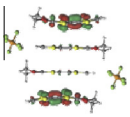	$\varepsilon = -0.2513$	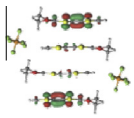
1*u* HOMO-1	$\varepsilon = -0.2783$	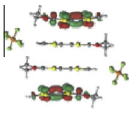	$\varepsilon = -0.2735$	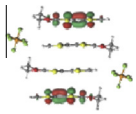
1*g* HOMO-2	$\varepsilon = -0.3010$	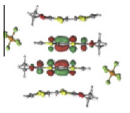	$\varepsilon = -0.2999$	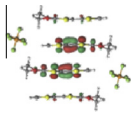
CO	0.04 0.88 0.88 0.04		0.14 0.79 0.79 0.14	

Besides the CS configuration, other low lying electronic configurations are also important for the analysis of the CASSCF calculations. We use ROHF to obtain their energies. Of special interest are the triplet and the open shell singlet states which, in the local basis, occupy the same local orbitals (${}^3_{OS}\psi$ and ${}^1_{OS}\psi$ in Table 1b).

In Table 7 the results of these ROHF calculations are summarised, in which we sequentially numbered the states in energy above the S_{0g} ground state. In both geometries, all calculated states have a ½½½½ charge distribution, except the T_{1u} and S_{1g} states that have a 0110 charge ordering. The CT to PF_6 is the same as in the CASSCF calculations. The diradical nature of the T_{1u} and S_{1g} states is apparent from the open shell orbitals (see Table 8). The open shell picture as sketched in Fig. 1 is obtained. The open shell S_{1g} ROHF state is mixed with the closed shell S_{0g} RHF state in the multi-configurational CASSCF singlet wave function (Section 4). We note that a strictly inversion symmetric nuclear potential is required to obtain this configuration. The charge hole localisation is similar to that in our RHF cluster calculations: 95% (86%) in the LT (HT) crystal. With T_{1u} and S_{1g} being lower in energy than S_{0g}, these states show triplet instability. We attribute the larger stabilisation of these states in the HT crystal to a larger separation of the inner molecules at HT.

Interestingly, in the HT crystal an open shell singlet state could be found in which one electron hole is localised on an inner EDO-TTF molecule and another one on an outer molecule, creating a 0101 charge ordering pattern. This open shell singlet state is 2 kcal/mol lower than the 0110 charge ordered S_{1g} state.

Table 7
ROHF open shell states obtained for different electronic configurations for the LT and HT cluster. Energies are relative to the S_{0g} RHF closed shell states in kcal/mol.

State	Configuration	E_{LT}	E_{HT}
S_{3g}	g^1g^1	46.6	24.8
T_{2g}	g^1g^1	46.4	24.6
S_{2g}	u^1u^1	19.3	7.4
T_{1g}	u^1u^1	19.2	7.2
S_{1u}	g^1u^1	18.5	6.1
S_{1g}	a^1b^1	−4.5	−14.3
T_{1u}	g^1u^1/a^1b^1	−4.7	−14.5

Table 8
Charge ordering and singly occupied open shell orbitals for the lowest open shell ROHF singlet S_{1g} and triplet T_{1u} state in the local basis $\{a, b\}$ representation.

	LT		HT	
	a^1	b^1	a^1	b^1
S_{1g}	 (0.04 0.89 0.89 0.04)		 (0.12 0.82 0.82 0.12)	
T_{1u}	 (0.04 0.89 0.89 0.04)		 (0.13 0.81 0.81 0.13)	

8. UHF cluster calculations

UHF cluster calculations show triplet instability, and spin contaminations are estimated from the total spin. These results provide an estimate of the spin contaminations found in the periodic states (Section 6) where we have been unable to calculate the total spin. The broken spin-symmetry ${}^{M_s=0}_{U}\psi$ UHF states we obtained for tetramer clusters are lower in energy (Table 9) than the corresponding closed shell states. The ${}^{M_s=1}_{U}\psi$ state is also below the closed shell state, just like the T_{1u} ROHF state (Table 7), which hints towards the mixing in of significant triplet character in the $M_s = 0$ UHF wave function. The values for the total spin $S(S+1)$ indicate spin-contamination. Assuming only contamination from the next higher multiplet, the percentage of contamination can be estimated in the following way. We use the normalised $\psi = \sqrt{1-x}^a\psi \pm \sqrt{x}^b\psi$ wave function, and with that the expectation value for the total spin can be written as $\psi|\widehat{S}^2|\psi = (1-x)^a\psi|\widehat{S}^2|^a\psi + x^b\psi|\widehat{S}^2|^b\psi$. For a $M_s = 0$ singlet ($a = 1$) mixed with a $M_s = 0$ triplet ($b = 3$) we find $x = 0.56$ (0.64) for the LT (HT) clusters. For the $M_s = 1$ triplet ($a = 3$) contaminated with a $M_s = 1$ quintet ($b = 5$) we get $x = 0.06$ (0.08) for LT (HT). Therefore the $M_s = 1$ state is mainly triplet and it contains a minor contamination of quintet. The large mixing of the $M_s = 0$ state can be understood from the triplet being lower in energy.

The CT to PF_6 in these states (Table 9) is equal to that of the CASSCF states. Also the charge hole localisation of 96% (92%) in the LT (HT) cluster is comparable to that in the CASSCF calculations. The outcome of the charge analysis for the $M_s = 0$ and $M_s = 1$ states are almost the same. The natural orbital population for the $M_s = 1$ states is $(n_g, n_u) = (1, 1)$, as expected. In the $M_s = 0$ states the natural orbital population is $(n_g, n_u) = (1.36, 0.64)$ for the LT cluster and $(n_g, n_u) = (1.22, 0.78)$ for the HT cluster. This indicates a 64% and 78% open shell singlet character respectively. Because the ${}^{1}_{OS}\psi(a,b)$ open shell singlet and the ${}^{3}_{OS}\psi(a,b)$ triplet wave functions can be seen as being built from the same local orbitals (Table 1b), the estimated 60% mixing in of the triplet causes this strong open shell character of the UHF $M_s = 0$ states.

The triplet instability in these UHF calculations is evident from the low lying $M_s = 1$ states. Iwano and Shimoi [9] too reported broken spin-symmetry states. They performed unrestricted DFT cluster calculations with designated embedding and obtained a state that is lower than a closed shell DFT solution by 6.9 kcal/mol for a system with 12 EDO-TTF molecules. Unfortunately no assessment was given for the spin contamination in their study.

Table 9
$M_s = 0$ and $M_s = 1$ UHF states for the LT and HT cluster in vacuum. Energy in kcal/mol is relative to the corresponding RHF state.

	M_s	E	$S(S+1)$	CO
LT	0	−15.2	1.11	(0.03 0.89 0.89 0.03)
	1	−18.9	2.24	(0.04 0.89 0.89 0.04)
HT	0	−15.0	1.27	(0.08 0.86 0.86 0.08)
	1	−20.3	2.31	(0.09 0.85 0.85 0.09)

9. Conclusion and discussion

The main issue addressed in this paper is whether the best ansatz for the ground state of the $(EDO\text{-}TTF)_2PF_6$ system is a closed-shell or open shell representation. Our periodic calculations, in which the whole crystal is explicitly described, show that the closed shell states are in agreement with experiment [2]. The nature of the conductivity and the charge ordering is reproduced in both the high temperature conducting state and the low temperature insulating state. This is underlined with the absence of experimentally observed magnetism, which makes it likely that the ferromagnetic state is not at very low energy. Results of our spin-unrestricted cluster and periodic calculations indicate however that there is triplet instability. Since there are no experimentally observed magnetic states, it is likely that these spin-polarised solutions do not describe the ground state. However, they indicate that the ground state has multi-determinantal character and that there might be instability towards a magnetic state. This may be different in other organic CT salts. Notably in the $TMTTF_2PF_6$ Fabre salt, a magnetic state exists under pressure and at low temperature [6]. We consider the term radical cation salts, which is sometimes used to classify Bechgaard and Fabre salts, not appropriate for the $(EDO\text{-}TTF)_2PF_6$ system.

We also obtained states with charge ordering patterns that are not observed experimentally or only as short lived intermediate states in photo induced phase transitions [22]. It shows the instability of the ground state towards states with other charge ordering patterns. Most notably we found a low lying 0110 charge ordered state with spin-restricted periodic Hartree–Fock theory in the HT crystal. The energy differences between these calculated states are smaller than can be expected to be reliably distinguished from these calculations. The relative order in energy of these solutions might also be sensitive to small variations in the geometry that fall within the accuracy of the X-ray diffraction experiments from which our geometries were obtained.

From the analysis of systematic cluster calculations performed with RHF, ROHF and CASSCF/CASCI theory, we have been able to discuss the electronic configurations that are important in these competing states. With R(O)HF we showed that the open shell singlet ${}^{1}_{OS}\psi$, the open shell triplet ${}^{3}_{OS}\psi$, and the closed shell singlet ${}^{1}_{CS}\psi$ of the tetramer are close in energy. Allowing several configurations to contribute to the wave function, our CASSCF results show clearly

that the ground state is singlet. This is also the case in embedded CASSCF calculations. Due to the proximity of the singlet and triplet states we expect that the singlet state has a considerable open shell character. The CASSCF singlet-triplet splitting is largest in the LT phase, which indicates a large electron interaction in a two electron picture. The CASSCF wave function in the HT phase shows the largest open shell character. It can be considered half way between a closed shell g^2 and open shell $g^2 - u^2$ wave function, which we attribute to the cluster effect of charge hole localisation.

In the cluster calculations, the positive charges localise in the interior of the HT cluster whereas in the crystal they are delocalised. We showed in our embedded calculations that this cannot be overcome by including the electrostatic effects of the environment. Essentially, these electrostatic effects on the quantum cluster showed to be negligible. Orbital and population analysis, show the tendency towards charge hole localisation. In the LT cluster we see a larger charge hole localisation than in the HT cluster where the dimers are at larger distance. Compared to RHF, the effect is enhanced by using UHF and CASSCF. In CASSCF the localisation of holes is increased by correlation: because of mixing in of an u^2 configuration in the wave function. Driving the electrons away from the centre, by occupying an ungerade orbital that is anti-bonding between the dimers, is expected to be effective in this process.

Acknowledgments

Remco Havenith is acknowledged for stimulating discussions and also for providing computational assistance. We thank Ibério de P.R. Moreira for his feedback on our results.

References

[1] J.B. Torrance, The difference between metallic and insulating salts of tetracyanoquinodimethane (TCNQ): how to design an organic metal, Acc. Chem. Res. 12 (3) (1979) 79–86.
[2] A. Ota, H. Yamochi, G. Saito, A novel metal–insulator phase transition observed in (EDO-TTF)$_2$PF$_6$, J. Mater. Chem. 12 (2002) 2600–2602.
[3] G.J. Linker, P.H.M. van Loosdrecht, P.Th. van Duijnen, R. Broer, Comparison of ab initio molecular properties of EDO-TTF with the properties of the (EDO-TTF)$_2$PF$_6$ crystal, Chem. Phys. Lett. 487 (2010) 220–225.
[4] S. Aoyagi, K. Kato, A. Ota, H. Yamochi, G. Saito, H. Suematsu, M. Sakata, M. Takata, Direct observation of bonding and charge ordering in (EDO-TTF)$_2$PF$_6$, Angew. Chem. Int. Ed. 43 (2004) 3670–3673.
[5] K. Kamada, K. Ohta, A. Shimizu, T. Kubo, R. Kishi, H. Takahashi, E. Botek, B. Champagne, M. Nakano, Singlet diradical character from experiment, J. Phys. Chem. Lett. 1 (2010) 937–940.
[6] J.P. Pouget, S. Ravy, X-ray evidence of charge density wave modulations in the magnetic phases of (TMTSF)$_2$PF$_6$ and (TMTTF)$_2$Br, Synth. Met. 85 (1997) 1523–1528.
[7] M. Dressel, M. Dumm, T. Knoblauch, B. Köhler, B. Salameh, S. Yasin, Charge order breaks magnetic symmetry in molecular quantum spin chains, Adv. Cond. Matter Phys. 2012 (2012) 398721.
[8] K. Iwano, Y. Shimoi, DFT calculations for the high-temperature structure of (EDO-TTF)$_2$PF$_6$: identification of an electronic molecular dimer, J. Phys: Conf. Ser. 148 (2009) 012010.
[9] K. Iwano, Y. Shimoi, Strong electron correlation in the high-temperature phase of (EDO-TTF)$_2$PF$_6$ as a quasi-one-dimensional molecular conductor, J. Phys. Soc. Jpn. 79 (10) (2010) 103705.
[10] K. Iwano, Y. Shimoi, Revealing the photorelaxation mechanism in a molecular solid using density-functional theory, Phys. Rev. Lett. 110 (2013) 116401.
[11] M. Filatov, Antiferromagnetic interactions in the quarter-filled organic conductor (EDO-TTF)$_2$PF$_6$, Phys. Chem. Chem. Phys. 13 (2011) 12328–12334.
[12] D. Dehareng, G. Dive, Hartree–Fock instabilities and electronic properties, J. Comput. Chem. 21 (6) (2000) 483–504.
[13] J. Čížek, J. Paldus, Stability conditions for the solutions of the Hartree–Fock equations for atomic and molecular systems. Application to the Pi electron model of cyclic polyenes, J. Chem. Phys 47 (1967) 3976–3985;
K. Yamaguchi, Generalized molecular orbital (GMO) theories of organic reaction mechanisms. Otbital symmetry, orbital stability and orbital pairing rules, Chem. Phys. 29 (1978) 117–139.
[14] M. Yamochi, S. Koshihara, Organic metal (EDO-TTF)$_2$PF$_6$ with multi-instability, Sci. Technol. Adv. Mater. 10 (2009) 024305.
[15] O. Drozdova, K. Yakushi, A. Ota, H. Yamochi, G. Saito, Spectroscopic study of the [0110] charge ordering in (EDO-TTF)$_2$PF$_6$, Synth. Met. 133–134 (2003) 277–279.
[16] P.M. Kozlovski, M. Dupuis, E.R. Davidson, The cope rearrangement revisited with multireference perturbation theory, J. Am. Chem. Soc. 117 (1995) 774–778.
[17] E.R. Davidson, The spatial extent of the v state of ethylene and its relation to dynamic correlation in the cope rearrangement, J. Phys. Chem. 100 (1996) 6161–6166.
[18] R. Lindth, M. Schütz, Singlet benzyne thermochemistry: a CASPT2 study of the enthalpies of formation, Chem. Phys. Lett. 258 (1996) 409–415.
[19] C.J. Cramer, J.J. Nash, R.R. Squires, A reinvestigation of singlet benzyne thermochemistry predicted by CASPT2, coupled-cluster and density functional calculations, Chem. Phys. Lett. 277 (1997) 311–320.
[20] M. Chollet, L. Guerin, N. Uchida, S. Fukaya, H. Shimoda, T. Ishikawa, K. Matsuda, T. Hasegawa, A. Ota, H. Yamochi, G. Saito, R. Tazaki, S. Adachi, S. Koshihara, Gigantic photoresponse in ¼-filled-band organic salt (EDO-TTF)$_2$PF$_6$, Science 307 (2005) 86–89.
[21] K. Onda, S. Ogihara, K. Yonemitsu, N. Maeshima, T. Ishikawa, Y. Okimoto, X. Shao, Y. Nakano, H. Yamochi, G. Saito, S. Koshihara, Photoinduced Change in the charge order pattern in the quarter-filled organic conductor EDO-TTF$_2$PF$_6$ with a strong electron-phonon interaction, Phys. Rev. Let. 101 (2008) 067403.
[22] B. Siwick, E. Collet, Molecular motion watched, Nature 496 (2013) 306–307.
[23] P.C. Hariharan, J.A. Pople, The influence of polarization functions on molecular orbital hydrogenation energies, Theor. Chim. Acta 28 (1973) 213–222;
M.M. Francl, W.J. Pietro, W.J. Hehre, J.S. Binkley, M.S. Gordon, D. DeFrees, J.A. Pople, Selfconsistent molecular orbital methods. XXIII. A polarization type basis set for second row elements, J. Chem. Phys. 77 (1982) 3654–3665.
[24] M.F. Guest, I.J. Bush, H.J.J. van Dam, P. Sherwood, J.M.H. Thomas, J.H. van Lenthe, R.W.A. Havenith, J. Kendrick, The GAMESS-UK electronic structure package: algorithms, developments and applications, Mol. Phys. 103 (6–8) (2005) 719–747.
[25] G. Karlström, R. Lindh, P. Malmqvist, B.O. Roos, U. Ryde, V. Veryazov, P. Widmark, M. Cossi, B. Schimmelpfennig, P. Neogrady, Luis Seijo, MOLCAS: a program package for computational chemistry, Comput. Mater. Sci. 28 (2003) 222–239.
[26] R. Dovesi, V.R. Saunders, C. Roetti, R. Orlando, C.M. Zicovich-Wilson, F. Pascale, B. Civalleri, K. Doll, N.M. Harrison, I.J. Bush, P. D'Arco, M. Llunell, CRYSTAL 2009 User's Manual, University of Torino, Torino, 2009.
[27] W.J. Hehre, L. Radom, P.R. Schleyer, J.A. Pople, Ab initio molecular orbital theory, 1986.
[28] R.S. Mulliken, Electronic population analysis on LCAO–MO molecular wave functions, J. Chem. Phys. 23 (1955) 1833–1840.
[29] M. Swart, P.Th. van Duijnen, J.G. Snijders, A charge analysis derived from an atomic multipole expansion, J. Comput. Chem. 22 (1) (2001) 79–88.
[30] M. Swart, P.Th. van Duijnen, DRF90: a polarizable force field, Mol. Simul. 32 (2006) 471–484.